Influence of the Morphology of the Oxide Supports on Catalytic Performances of V/SiO_2 and V/MgO Catalysts in Methanol Partial Oxidation

Yu-Chuan Lin and Keith L. Hohn*

Department of Chemical Engineering, Kansas State University, Manhattan, KS 66506, USA

1. Introduction

Various unique properties have been observed on nanoscale materials, including novel magnetism, optical, melting points, surface chemistry, mechanical and metallic behavior [1]. These properties have ignited the development of nanotechnology in last decade. In metal oxide catalysts, major effort has paid on the investigation of nanometer-sized active sites dispersed on the supports such as Au nanoparticles on TiO_2 in oxidation of CO [2] or nanoscale CeO_2 for reduction SO_2 by CO [3]. Nevertheless, discussion of the morphology effects on catalytic reactions from nanocrystalline and microcrystalline supports is lacking, though it is believed that the interaction between the active phase and support may drive the reaction in different ways [4].

To reveal the influence of supports with different crystal sizes, both nano- and micro-scale supports should be prepared. Sol-gel techniques have been reported to produce metal oxides with crystal sizes of only nanometers [5], and these metal oxides have been found to have different chemical and catalytic properties than conventional metal oxides [1]. For example, the surface hydroxyls on sol-gel prepared MgO have been found to be concentrated on edge and corner and are less acidic than on conventional MgO [1]. This may lead to an unusual structure of active phases and different catalytic results.

The support morphology may change the acid-base properties or redox properties of the resulting supported catalyst. This would be analogous to how different metal oxides (i.e. MgO vs. TiO_2) lead to different chemical properties that affect catalyst activity. Support morphology may also lead to differences in the supported phase or phases due to the increased surface area of the nanocrystalline supports. This paper studies how the use of two aerogel-prepared (AP) metal oxides (SiO_2 and MgO) as supports for vanadium affects the vanadium surface phases and the chemical properties of the catalysts.

Methanol partial oxidation, an effective way to characterize both structural and chemical properties of oxide catalysts [6], has been employed in this study; while H_2-TPR is used to evaluate the reducibility of the catalysts. Several techniques were also used to characterize

the physical properties of the catalysts (BET, Raman spectroscopy, and UV-Vis spectroscopy).

This report also looks at how turnover frequency in methanol oxidation varies as a function of vanadium weight loading. Bell and co-workers recently reported that vanadium surface density played an important role in oxidative dehydrogenation, where bridging vanadate groups led to less active phase than smaller ones [7]. Therefore, important mechanistic information can be obtained by understanding how turnover frequency varies with vanadium weight loading. Using sol-gel prepared SiO_2 and MgO offers a mean for investigating this question because their high surface areas should allow more vanadium to be loaded without forming bulk phases.

2. Experimental Section

2.1 Catalyst Preparation

Two types of SiO_2 and MgO were applied in this study: conventionally prepared (CP) and aerogel prepared (AP) silicon and magnesium oxides. CP SiO_2 was purchased from Degussa (Aerosoil-380, S_{BET} = 367 m^2/g), and pretreated with water to allow easy handling. CP MgO was prepared by pretreating commercially purchased MgO (Aldrich, 99+ %) in boiling water overnight with stirring. After cooling and filtering, the paste of magnesium hydroxide was dried in an oven at 120 ^oC for 2 hours and then calcined at 500 ^oC under vacuum overnight.

AP SiO_2 and MgO were formed by a sol-gel process combining with supercritical drying in a bench-top autoclave (Parr Model 4843) [1]. The sol-gel synthesis procedures were described elsewhere [1,5].

Vanadium was then introduced onto each support by the incipient-wetness method [8]. Various vanadium weight loadings, from 0.5 to 10 % of V/SiO_2 and 5 to 30 % of V/MgO, were prepared using both AP and CP supports. Also 15 and 30 % weight loadings of CP V/SiO_2 catalysts were synthesized to investigate the surface V_2O_5 phase and its catalytic performance.

2.2 Catalyst Characterization

The surface areas of all samples were measured by a Quantachrome NOVA 1200 instrument. Before each run, approximately 0.1 g of catalyst was degassed at 300 ^oC for 30

minutes. Six-point BET surface areas were calculated from the nitrogen adsorption isotherms.

Raman spectra were obtained by a Chromex Raman 2000 instrument in 200-2000 cm^{-1} wavelength range with 785 nm laser beam. Ground samples were packed within plastic cuvettes and placed inside a cuvette holder (Quantum Northwest TLC 50) for spectra collections.

Temperature-programmed reduction of hydrogen was measured in an Altamira AMI-200 system. 0.2 g samples were loaded in a quartz U-tube reactor and treated at 550 ^oC for 1 hour in pure O_2 to fully oxidize the samples. After cooling, the temperature was ramped from 50 ^oC to 850 ^oC at a constant rate of 5 ^oC/min in a flow of 5 % H_2 in Ar. H_2 consumption was monitored using a thermal conductivity detector (TCD).

UV-Vis spectra were acquired by a Varian-Cary 500 Scan UV–Vis NIR spectrophotometer with an integrating sphere attachment in the 1.5 to 6.2 eV photon energy range. The absorption spectra were acquired by using Teflon powder as a reference. The adsorption edge energy was measured by a least-squares fit of a line through a low energy edge of an absorption spectrum [9,10]

2.3 Catalytic Reactivity Testing

Methanol partial oxidation was applied as a chemical probe of both CP- and AP- V/SiO_2 and V/MgO catalysts. Detail setup was described in a prior publication [11]. About 0.06 gram of catalyst was used in this study instead of 1 gram. Both oxygen (99.0 %) and nitrogen (97.0+ %) were obtained from Linweld. Methanol (99.9 %) was obtained from Fisher. All gases were used without further purification. Methanol was introduced into the system by a syringe pump (New Era NE-500) with a 0.01 mL/min injection rate. Gas flows of oxygen and nitrogen were regulated by mass flow controllers (Brooks Instrument, 5850E) and blended with methanol vapor to achieve a 13/81/6 (mole %) mixture. The total flow rate was around 100 standard cubic centimeters per minute (sccm).

Before each run, samples were pretreated at 450 ^oC for 30 minutes in a stream of oxygen and nitrogen. Catalytic results were acquired at 250 ^oC for V/SiO_2 catalysts and 150 ^oC for V/MgO catalysts, beginning 20 minutes after injection of methanol through the system. Blank runs were performed in the reactor with packed quartz wool without any detectable conversion of methanol.

For all data reported, the carbon and hydrogen mass balances closed within 10 % error and most within 5 %. For each sample, three to five trials were run to determine reproducibility. These multiple trials were used to estimate 95 % confidence intervals for catalytic activity, selectivity and turnover frequency (TOF). Activity was calculated from conversion: the number of moles of methanol converted per hour per gram catalyst (mole/hr×g), noted as Ac. The selectivity (%) of product X_i is calculated as 100 × (number of moles methanol converted to product X_i)/(total number of moles of methanol converted). Turnover frequency (s^{-1}), defined as the moles of methanol converted per surface vanadium atom per second [4], was found by dividing activity by the number of active sites per gram of catalyst. The number of active sites was calculated from the number of vanadium atoms, found from the nominal weight loading.

3. Results

3.1 Physical Property

Table 1 and 2 present the surface areas, calculated surface vanadia densities and UV-Vis absorption edge energies of all AP and CP V/SiO_2 and V/MgO catalysts. Surface densities of vanadium atoms were calculated from the nominal vanadia loading values. A decreasing trend of surface area has been found with increased vanadium doping, with only a few exceptions. Surface areas of all AP catalysts are at least twice as high as CP catalysts. This leads to lower the surface densities for AP catalysts at all loadings.

Table 1

wt%	AP V/SiO_2			CP V/SiO_2		
	Surface area (m^2/g)	Surface density (VO_x/nm^2)	Absorption edge energy (eV)	Surface area (m^2/g)	Surface density (VO_x/nm^2)	Absorption edge energy (eV)
0	760.9	0		270.6	0	
0.5	772.1	0.04	2.20	268.6	0.12	2.11
1	742.3	0.09	2.15	260.5	0.25	2.08
2	716.6	0.18	2.10	268.1	0.48	2.00
3	618.1	0.31	2.05	262.1	0.74	2.01
5	564.3	0.56	2.07	244.1	1.29	1.91
7	551.1	0.79	2.03	240.6	1.80	1.89
10	566.0	1.06	2.03	206.4	2.92	1.89

Table 2

wt%	AP V/MgO			CP V/MgO		
	Surface area (m^2/g)	Surface density (VO_x/nm^2)	Absorption edge energy (eV)	Surface area (m^2/g)	Surface density (VO_x/nm^2)	Absorption edge energy (eV)
0	285.0	0		126.1	0	
5	263.4	1.2	2.75	124.2	2.5	2.75
10	266.2	2.3	2.70	114.2	5.3	2.65
15	252.0	3.4	2.68	88.3	9.8	2.68
20	224.7	4.9	2.75	88.9	12.4	2.65
25	206.3	6.4	2.64	76.6	17.3	2.59
30	156.3	9.8	2.65	70.3	21.7	2.49

3.2 Raman Spectroscopy

V/SiO_2

Figure 1 shows the Raman spectra of hydrated AP and CP V/SiO_2 catalysts with 0, 1, 3, 5, and 10 % of vanadia weight loadings. In addition, the spectrum of crystalline vanadium pentoxide is shown as a reference. Neither AP nor CP samples give characteristic peaks of V_2O_5 crystals or isolated VO_4 groups, which has been reported to locate at around $1000cm^{-1}$.

A small but clear peak appears at 1037 cm^{-1} for CP V/SiO_2 catalysts when vanadium loading is increased to 10 %. According to previous researchers, $V_2O_5 \cdot nH_2O$ gels were formed as hydrated V-O-Si bonds in isolated $(SiO)_3V{=}O$ groups resembling together and its Raman spectra holds the peak at 1021 cm^{-1} [12]. Thus, it is reasonable to assume that the weak peak located in our Raman spectrum for 10 % CP V/SiO_2 is due to $V_2O_5 \cdot nH_2O$ gels. This index peak is marked with an asterisk in Figure 1.

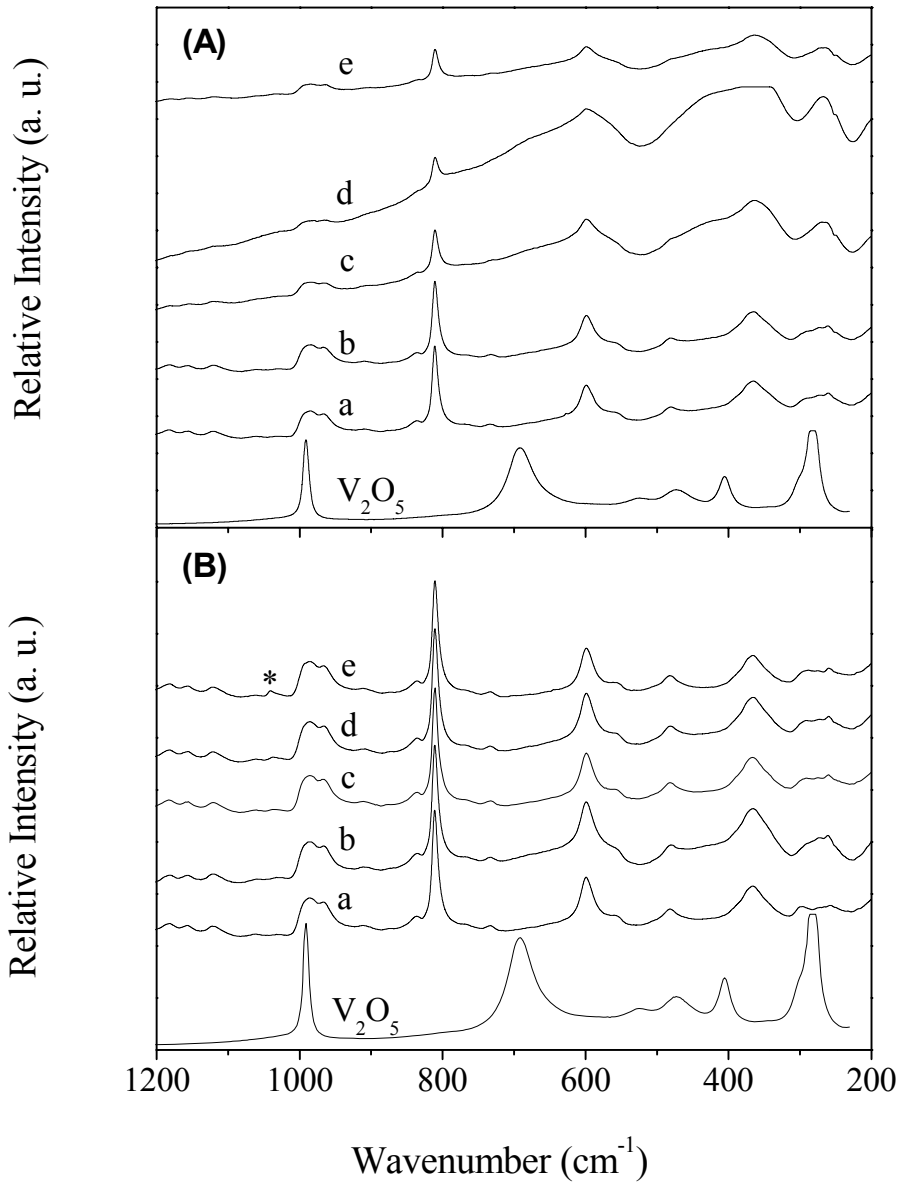

Figure 1. Raman spectra for hydrated (A) AP V/SiO_2 and (B) CP V/SiO_2 with (a) 0 %, (b) 1 %, (c) 3 %, (d) 5 %, and (e) 10 % V_2O_5 weight loadings at 200-1200 cm^{-1} range. Noted the asterisk (*) indicates the index peak of $V_2O_5 \bullet nH_2O$ gels.

V/MgO

Figure 2 presents the Raman spectra of AP and CP V/MgO catalysts with vanadium weight loadings of 0, 5, 10, 20, 25, and 30 %. Reference phases, including $Mg_3(VO_4)_2$, $Mg_2V_2O_7$ and V_2O_5, were also collected under the same conditions. None of these references are apparent between 0 to 10 %. At vanadium weight loadings of 20 % and above, both AP and CP V/MgO catalysts exhibit a strong peak at ~860 cm^{-1}, which can be ascribed to the V-O bond stretching vibration in $Mg_3(VO_4)_2$. The characteristic peaks of $Mg_2V_2O_7$ were not present in any AP V/MgO catalysts; in contrast, a sharp peak at 951 cm^{-1} assigned to magnesium pyrovanadate has been found for 25 and 30 % CP V/MgO.

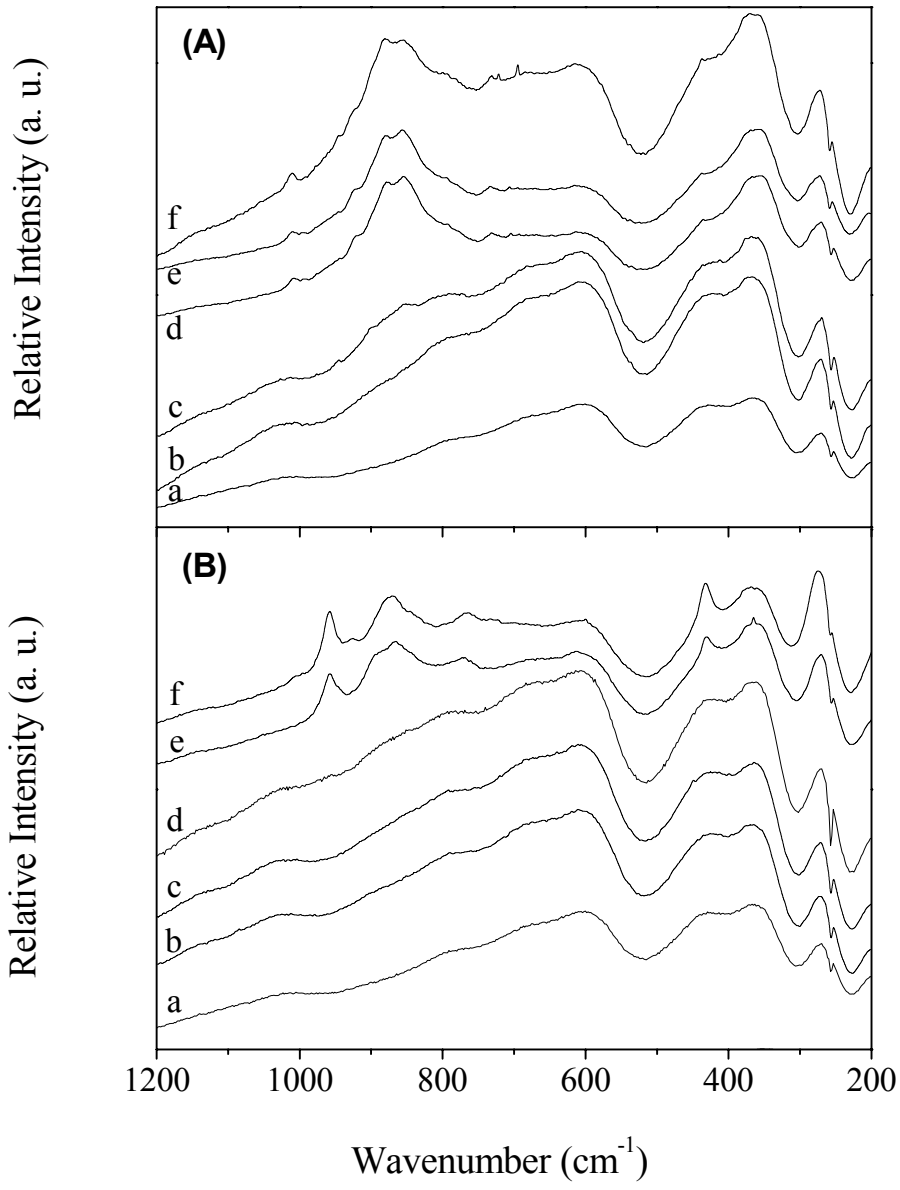

Figure 2. Raman spectra for hydrated (A) AP V/MgO and (B) CP V/MgO with (a) 0 %, (b) 5 %, (c) 10 %, (d) 20 %, (e) 25 % and (f) 30 % vanadia weight loadings at 200-1200 cm^{-1} range.

3.3 H_2 Temperature-Programmed Reduction

V/SiO_2

Only one reduction peaks has been observed for each H_2 TPR profile for 1, 3, 5, and 10 % vanadia loadings on AP and CP silica supports. The peak where the amount of H_2 consumption is maximum, noted as T_{max}, increased with increased loading and was similar for AP and CP V/SiO_2 catalysts. The T_{max} for 1, 3, 5 and 10 % AP V/SiO_2 locate at 507, 537, 538, and 576 ^oC, while 1, 3, 5 and 10 % CP V/SiO_2 hold T_{max} at 508, 519, 540, and 580 ^oC. One broad peak may enclose multiple peaks from several surface vanadyl phases [13]. According to previous work, crystalline V_2O_5 on silica possesses the highest T_{max} of any vanadyl species [4,14,15]. Thus, it may imply that at higher vanadia loadings, there is more V_2O_5 on the silica surface.

V/MgO

For 0, 10, 20, and 30 % vanadia loadings on AP and CP magnesia supports, only one peak was observed for each sample except for pure AP and CP MgO, which had no reduction peaks. The T_{max} of 10, 20 and 30 % AP V/MgO are at 661, 676 and 708 ^oC, while 10, 20 and 30 % CP V/MgO exhibit T_{max} at 651, 698 and 748 ^oC. The asymmetric shape (shoulder) of each peak on the low-temperature side suggested that there were at least two types of vanadia phases inside the catalyst [16,17].

A linear trend between vanadia loadings and detected hydrogen consumptions has been observed for both AP and CP V/SiO_2 and V/MgO samples. Moreover, the difference of H_2 consumption between AP and CP samples were within 10 % variance with the same vanadium weight loading. This suggests that the actual vanadium loadings are close to the nominal values.

3.4 UV-Vis Diffuse Reflectance

Figure 3 shows the UV-Vis spectra of 1, 5 and 10 % AP and CP V/SiO_2. V_2O_5, used as a reference, possesses three absorption bands in the 500-400, 400-300 and 300-200 nm regions, is also included in this figure. The absorption bands of V_2O_5 have not been

observed in AP samples. On the contrary, higher loading CP samples, including 5 and 10 %, exhibit a shoulder near 500 nm. This may be the evidence of the presence of V_2O_5. Table 1 and 2 exhibit the dependence of UV-Visible absorption edge energy on various vanadia loadings of both AP and CP V/SiO_2 and V/MgO. The absorption edge energies were measured by the x-intercept of a linear fit of a line through the transformed absorption spectra. More detail about these procedures was described elsewhere [11]. A recent article discussing the relation between the absorption edge energy and size of surface oxide domains noted that the bandgap energy of a real system decreases as the domain size increases [18]. Therefore, the decreasing absorption edge energies with increasing vanadia contents shown in Table 1 and 2 implies that the size of the two-dimensional active oxide domains grows [9]. Moreover, AP catalysts possess higher edge energies than CP catalysts for both V/SiO_2 and V/MgO at almost all loadings with several exceptions. This suggests that surface vanadia phases on AP supports were smaller than those on CP supports.

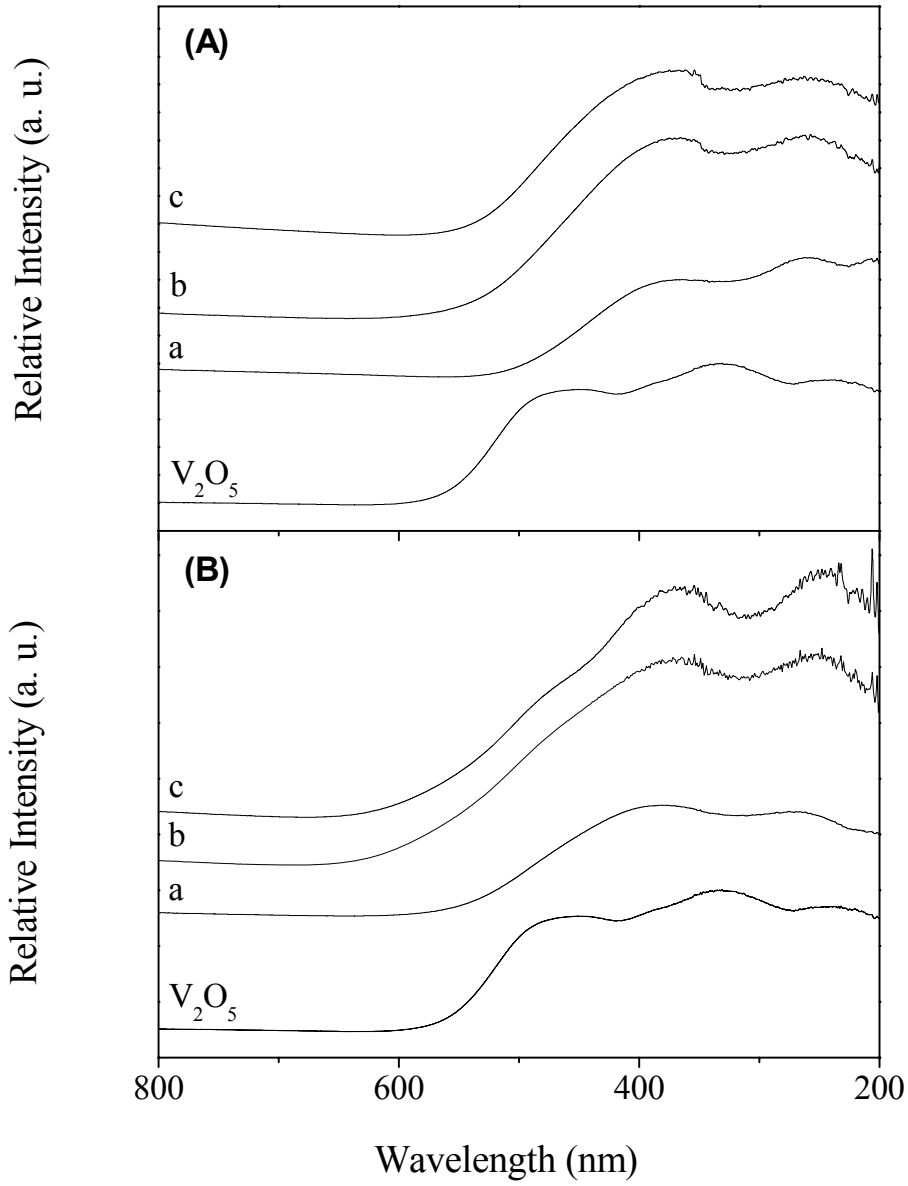

Figure 3. UV-Visible diffraction spectra for (A) AP V/MgO and (B) CP V/MgO with (a) 1 %, (b) 5 % and (c) 10 % vanadia weight loadings.

3.5 Catalytic Studies

V/SiO$_2$

Table 3 and 4 summarize the reactivities for methanol partial oxidation at 250 ^{o}C of AP and CP V/SiO$_2$ catalysts. Pure AP and CP silica were utilized as references and both of them produce CO_x (carbon dioxides and carbon monoxide), dimethyl ether, and water.

Other products, including formaldehyde, methyl formate, and dimethoxy methane, were generated when supported vanadium oxides were involved in the reaction.

AP catalysts show similar activity to CP catalysts for weight loadings less than 3 %, but higher activity at weight loadings of 3 % or higher on the basis of vanadium weight loading. However, comparing activity on a vanadium surface density basis, as is done in Figure 4, changes the trend. Both AP and CP catalysts have nearly the same activity at all vanadium surface densities.

Table 3

AP	Ac	Selectivity (%)				
wt. %	$\left(\frac{\text{mole MeOH conv.}}{\text{g} \cdot \text{hr}}\right)$	CO_x	FA	DME	MF	DMM
0	9.8×10^{-3}	89	0	11	0	0
0.5	1.5×10^{-2}	30	60	4	5	1
1	1.4×10^{-2}	25	61	7	6	1
2	1.9×10^{-2}	26	63	4	5	2
3	3.1×10^{-2}	9	83	4	2	2
5	5.2×10^{-2}	9	82	3	2	1
7	6.5×10^{-2}	8	84	3	2	3
10	7.1×10^{-2}	8	84	3	2	3

Table 4

CP	Ac	Selectivity (%)				
wt. %	$\left(\frac{\text{mole MeOH conv.}}{\text{g} \cdot \text{hr}}\right)$	CO_x	FA	DME	MF	DMM
0	3.7×10^{-3}	84	0	16	0	0
0.5	9.0×10^{-3}	26	62	5	6	1
1	1.4×10^{-2}	14	73	6	6	1
2	1.8×10^{-2}	17	70	6	5	2
3	2.5×10^{-2}	8	83	4	3	2
5	3.3×10^{-2}	5	86	4	2	3
7	5.5×10^{-2}	8	82	5	2	3
10	5.3×10^{-2}	7	81	7	2	3

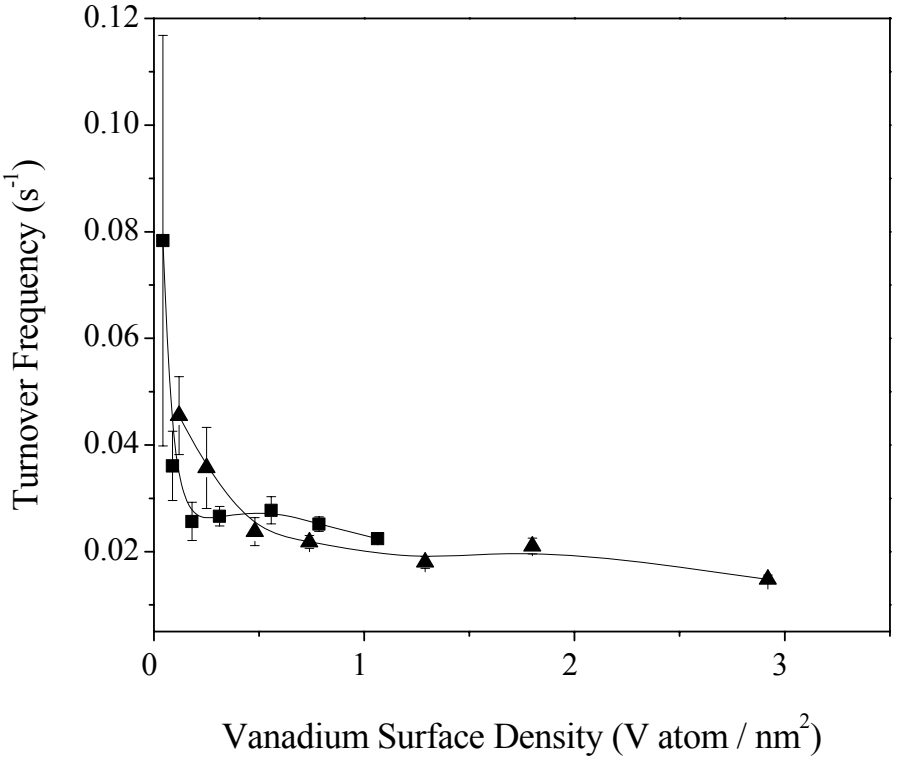

Figure 4. Turnover frequency (s^{-1}) for AP V/SiO_2 (■) and CP V/SiO_2 (▲) with different vanadia surface densities.

V/MgO

Table 5 and 6 list the selectivity and activity of both AP and CP V/MgO catalysts in methanol partial oxidation, respectively. Pure AP and CP magnesia were applied as references and both produced carbon oxides, formaldehyde, and methyl formate. After introducing vanadium, other products, including dimethyl ether and dimethoxy methane, were formed. As seen in Table 5 and 6, on a weight % basis, AP V/MgO was more active at 10 % weight loadings and higher. However, when TOF is compared as a function of vanadia surface density, as shown in Figure 5, both catalysts have roughly the same TOF.

Table 5

AP	Ac	Selectivity (%)				
wt. %	$\left(\frac{\text{mole MeOH conv.}}{\text{g} \cdot \text{hr}}\right)$	CO_x	FA	DME	MF	DMM
0	6.7×10^{-3}	27	67	0	6	0
5	1.8×10^{-2}	6	76	7	8	3
10	2.7×10^{-2}	7	77	5	8	3
15	2.7×10^{-2}	5	75	4	11	5
20	3.5×10^{-2}	5	75	4	11	5
25	3.9×10^{-2}	4	77	4	11	4
30	4.4×10^{-2}	6	81	3	8	2

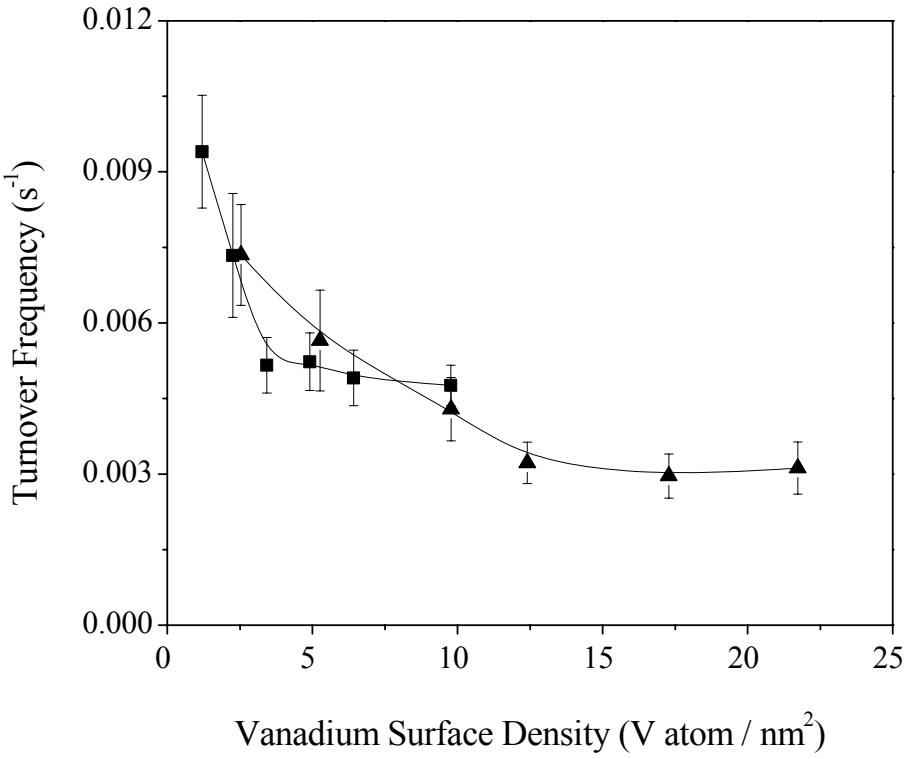

Figure 5. Turnover frequency (s^{-1}) for AP V/MgO (■) and CP V/MgO (▲) with different vanadia surface densities.

4. Discussion

4.1. Catalyst Structure

Both types of catalysts were analyzed by Raman, UV-Vis, and H_2-TPR to probe the surface configurations of vanadium oxides on SiO_2 and MgO. Of primary interest is whether polymeric vanadium phases form, the size of vanadium domains and how the formation of these phases varies between AP and CP supports.

V/SiO_2

It is reasonable to assume monometric vanadyl groups dominate on silica surface at low loading (< 3 %). This is proved by the white color of dehydrated V/SiO_2 because isolated vanadyl groups are colorless and silica possesses white color. The absence of features of V_2O_5 or $V_2O_5 \cdot nH_2O$ in the Raman spectra also suggest monomeric vanadyl groups, though peaks associated with monomeric vanadyl groups were not seen. With increased loading, polymetric vanadyl groups are expected. The darker colors of high weight loading dehydrated samples indicate the formation of V_2O_5, which has a deep orange color. Though the characteristic peak of V_2O_5 at 990 cm^{-1} was not seen, a small but clear peak belongs to $V_2O_5 \cdot nH_2O$ at 1037cm^{-1} was observed. This may be the hydration of both monovanadate and/or pyrovanadate to form this gel-like structure [12] H_2 TPR results show climbing T_{max} with enhanced vanadium doping. Since V_2O_5 has a higher reduction temperature than vanadyl groups, this may evidence an increasing presence of V_2O_5 as weight loading is increased. The UV-Vis spectra also point out a shoulder of higher loading CP samples close to the index band of V_2O_5, which suggests the existence of V_2O_5.

V/MgO

Though isolated or small domains of vanadates are expected, there is no characteristic peaks from ortho- or pyrovanatate in 10 % or lower loadings of V/MgO catalysts. At higher vanadia dopings, orthovanadate were found on AP V/MgO and both ortho- and pyro-vanadate were seen on CP V/MgO. No V_2O_5 has been detected for either series. According to previous studies, with an increase of vanadia contents, $Mg_3(VO_4)_2$ was the first component detected, then both $Mg_3(VO_4)_2$ and $Mg_2V_2O_7$ were seen. When more vanadia was doped, crystalline V_2O_5 was present [19,20]. This could be the evidence that AP MgO, which possess about three times higher surface area than CP MgO, could sustain more small domains of vanadyl groups than CP MgO. Moreover, this could be attributed to the difference of surface chemistry. It was confirmed by Klabunde's group that AP MgO holds less acidic hydroxyl groups than CP MgO, which favors the interaction with acidic vanadia, and caused less polymetric vanadate to form.

4.2. Catalyst Selectivity and Reactivity

V/SiO_2

Methanol partial oxidation is a useful probe reaction for comparing chemical properties of different supports [4]. For instance, the types of catalytic sites (redox, acidic and basic) can be probed by observing the products formed [6]. For both AP and CP V/SiO_2, selectivites of products are close except at low weight loadings (0.5-2 %).CP samples hold higher formaldehyde and lower carbon oxides selectivity than AP samples. This margin may be attributed to the silica supports, rather than differences in surface vanadyl groups, since isolated monovanadate are expected on both types of silica at low vanadium loadings. This can be explained that AP silica, which has much higher surface area than CP silica, may allow more surface hyroxyls sites (Brønsted acid) to involve in the reaction by producing more carbon oxides and causing the decrease of selectivity to formaldehyde.

On the contrary, activities of both series show no difference at low loadings but a significant margin at high loadings. There are two possible explanations: First, the difference is caused by the reducibility of the metal-oxygen-vanadium bond; second, the configurations of surface vanadyl groups on these two types of silica are not the same.

If the reducibility of Si-O-V bond is not the same, the difference in TOF and results of H2-TPR should be clear. This is not the case: TOF of AP and CP catalysts are very close at almost all weight loadings and Tmax of AP and CP catalysts are within 5 ^oC of each other for all weight loadings, with the exception of 3 % samples where a 18 ^oC difference is found.

It is, therefore, hypothesized that the difference in activity is due to differences in the vanadium phases present at high weight loadings on AP and CP catalysts. This would be consistent with the observation that TOF is essentially the same for AP and CP at weight loadings less than 3 %: only monovanadate should be present on both catalysts. It is hypothesized that CP catalysts have more V_2O_5 present at the same weight than AP catalysts. This increased amount of V_2O_5 is thought to lower the activity of CP catalysts relative to AP catalysts.

This hypothesis assumes that V_2O_5 is less active than monovanadate species. This is counter to the trend that Wachs and Deo suggest [4], but in agreement with results reported by Koranne, et al. [21] who found that monovanadate on V/SiO_2 catalysts was more active than bulk V_2O_5 in the partial oxidation of methane.

Our results in Figure 4 show a decrease in TOF as the V_2O_5 weight percent is increased on both AP and CP V/SiO_2. This is consistent with aggregated phases being less active than isolated monovanadate species.

V/MgO

The selectivity between AP and CP catalysts are very close but AP V/MgO catalysts show higher activity than CP samples at 20% and higher loadings. If we look down to the intrinsic activity, TOF, for both samples, both trends are overlapped. It is assume that with the identical surface density, there is no difference between surface magnesium vanadate groups on AP and CP MgO, which resulted in the close TOF values. The decrease of TOF also indicated that the intrinsic activity of V/MgO catalyst is controlled by surface vanadia phases: The larger the magnesium vanadate groups, the less active the catalyst is. Thus, therefore, we probably can conclude that small domains of vanadyl groups on magnesia support are more active than magnesium vanadate clusters.

According to the results, we may assume that sol gel prepared oxide supports are able to disperse surface vanadyl groups as monovanadate phases than conventional oxide supports, on which polymetric or bulk phases are located.

Another interesting trend is TOF, the intrinsic activity of catalyst. A decreasing trend was observed for both types of catalysts with increasing vanadium doping. Since isolated vanadyl groups are likely formed at low vanadium loadings and polymetric or bulk phases are formed at high vanadium loadings, this may imply that isolated vanadyl groups are more active in methanol partial oxidation.

5. Conclusion

The catalytic differences between AP and CP V/SiO_2 and V/MgO catalysts are primarily explained by the higher surface area of AP supports. Due to these high surface areas, AP supports allow more disperse vanadium phases to form. It is hypothesized that these dispersed phases are more active than polymeric or bulk phases, which leads to the greated activity, per gram, noted when AP supports were used.

6. Acknowledgements

The authors express their appreciation to Professor Israel E. Wachs and Edward Lee of Lehigh University for research advice. The authors also acknowledge Professor Russell

C. Middaugh and Nick Harn of University of Kansas for assistance in acquiring all Raman spectra. The authors also thank Dr. Kenneth J. Klabunde and Johanna Häggström of Kansas State University for the collection of all UV-vis spectra. This work was supported by DOE EPSCOR Grant DE-FG02-01ER45896.

References

[1] K.J. Klabunde, J. Stark, O. Koper, C. Mohs, D.G. Park, S. Decker, Y. Jiang, I. Lagadic, and D. Zhang, J. Phys. Chem. 100 (1996) 12142.
[2] M. Valden, X. Lai and D.W. Goodman, Science 281 (1998) 1647.
[3] A. Tschope, J.Y. Ying, in:G.C. Hadjipanayis, R.W. Siegel (Eds.), Nanophase Materilas: Synthesis-Properties-Applications, Kluwer Academic, Dordrecht, The Netherlands, 1994, 781.
[4] G. Deo and I.E. Wachs, J. Catal. 146 (1994) 323.
[5] M.L. Anderson, C.A. Morris, R.M. Stroud, C.I. Merzbacher and D.R. Rolison, Langmuir 15 (1999), 674.
[6] J.M. Tatibouët, Appl. Catal. A 148 (1997) 213.
[7] C. Pak, A.T. Bell and T.D. Tilley, J. Catal. 206 (2002) 49.
[8] X. Gao, S.R. Bare, J.L.G. Fierro, M.A. Banares and I.E. Wachs, J. Phys. Chem. B 102 (1998) 5653.
[9] K. Chen, A.T. Bell and E. Iglesia, J. Catal. 209 (2002) 35.
[10] D.G. Barton, M. Shtein, R.D. Wilson, S.L. Soled and E. Iglesia, J. Phys. Chem. B 103 (1999) 630.
[11] R. Vidal-Michel and K.L. Hohn, J. Catal. 221 (2004) 127.
[12] S. Xie, E. Iglesia and A.T. Bell, Langmuir 16 (2000) 7162.
[13] G. Deo, I.E. Wachs and J. Haber, Cri. Rev. Surf. Chem. 4 (1994) 141.
[14] F. Roozeboom, M.C. Mittelmeijer-Hazeleger, J.A. Moulijn, J. Medema, V.H.J. De Beer and P.J. Gellings, J. Phys. Chem. 84 (1980) 2783.
[15] M.M. Koranne, J.G. Goodwin, Jr. and G. Marcelin, J. Catal. 148 (1994) 369.
[16] T. Blasco, J.M. López Nieto, A. Dejoz and M.I. Vazquez, J. Catal. 157 (1995) 271.
[17] F. Arena, F. Frusteri, and A. Parmaliana, Appl. Catal. A. 176 (1999) 189.
[18] R.S. Weber, J. Catal. 151 (1995) 470.
[19] T. Blasco and J.M. López Nieto, Appl. Catal. A 157 (1997) 117.
[20] X. Gao, P. Ruiz, Q. Xin, X. Guo and B. Delmon, J. Catal. 148 (1994) 56.
[21] M.M. Koranne, J.G. Goodwin, Jr. and G. Marcelin, J. Catal. 148 (1994) 388.